Peroxo-Bridged Dinuclear Cobalt(III) Complexes Containing *N*-Glycoside Ligands from Tris(2-aminoethyl)amine and D-Glucose or Maltose

Tomoaki Tanase,*,† Tomoko Onaka,† Masako Nakagoshi,† Isamu Kinoshita,‡ Kozo Shibata,‡ Matsumi Doe,‡ Junko Fujii,‡ and Shigenobu Yano*,†

Department of Chemistry, Faculty of Science, Nara Women's University, Nara 630-8285, Japan, and Department of Chemistry, Faculty of Science, Osaka City University, Sumiyoshi-ku, Osaka 558-8585, Japan

Received August 5, 1998

Peroxo-bridged dinuclear cobalt(III) complexes, $[\{Co((D\text{-}Glc)_2\text{-}tren)\}_2(\mu\text{-}O_2)]X_3\cdot 5H_2O$ (X = Cl (**2**·$5H_2O$), Br (**3**·$5H_2O$)) and $[\{Co((Mal)_2\text{-}tren)\}_2(\mu\text{-}O_2)]Cl_3\cdot 6H_2O$ (**4**·$6H_2O$), were prepared from $CoX_2\cdot 6H_2O$, tris(2-aminoethyl)-amine, and D-glucose (D-Glc) or maltose (α-D-glucopyranosyl-(1→4)-D-glucose; Mal), and were characterized by elemental analysis, UV−vis absorption, circular dichroism, ^1H and ^{13}C NMR spectroscopic techniques, and X-ray absorption and crystallographic analyses, where $(aldose)_2$-tren is bis(*N*-aldosyl-2-aminoethyl)(2-aminoethyl)amine (aldose = D-Glc, Mal). The structure of **2** and **4** were determined by X-ray crystallography to consist of two Co(III) ions bridged by a peroxo unit: **2**·$4H_2O\cdot CH_3OH$, orthorhombic, $P2_12_12_1$ (No. 19), $a = 19.384(8)$ Å, $b = 23.468(5)$ Å, $c = 13.195(5)$ Å, $V = 6002(2)$ Å^3, $Z = 4$, $D_{calcd} = 1.440$ g cm^{-3}, $T = -99$ °C, $R = 0.078$, $R_w = 0.085$ for 4961 reflections with $I > 3\sigma(I)$; **4**·$2.25H_2O\cdot 3.75CH_3OH$, monoclinic, $P2_1$ (No. 4), $a = 12.819(7)$ Å, $b = 49.168(18)$ Å, $c = 14.973(6)$ Å, $\beta = 104.59(4)°$, $V = 9130(7)$ Å^3, $Z = 4$, $D_{calcd} = 1.459$ gcm^{-3}, $T = -136$ °C, $R = 0.101$ for 6837 reflections with $I > 2\sigma(I)$. The hydrogen bondings between the sugar moieties deviates the Co−O−O−Co torsional angle from planarity to 100.4(6)° (**2**) and av 102(1)° (**4**). The electronic structures of the twisted $Co_2(\mu\text{-}O)_2$ core were discussed on the basis of extended Hückel MO calculations. The present discrete complexes have a tetravalent sugar domain around the dinuclear center and clearly demonstrated distinct sugar−sugar interactions which could be a minimal model for so-called sugar clusters of glycoproteins on cell surfaces.

Introduction

Interactions of carbohydrates with metal ions have been recognized as of potential importance in the bioinorganic field, since many sugar-processing enzymes have been revealed to function with redox nonactive metal ions such as Mg^{2+}, Mn^{2+}, and Zn^{2+} in the active sites.[1−8] Elucidation of reactivity and behavior of sugars around redox active metal ions also involves potential importance in relevance to ribonucleotide reductases which utilize nonhem diiron or coenzyme B_{12} functional unit.[9] However, the detailed synthetic and structural studies on sugar−metal complexes have been still limited due to their complicated stereochemistry, multifunctionality, and hygroscopic nature.

We have systematically studied the synthesis, characterization, and reactions of sugar−transition metal complexes in which carbohydrate moieties are anchored onto metal centers as *N*-glycosides with diamines.[10−27] A polyamine, tris(2-aminoethyl)amine (tren), has recently been used instead of diamines

† Nara Women's University.

‡ Osaka City University.

(1) Gracy, R. W.; Noltmann, E. A. *J. Biol. Chem.* **1968**, *243*, 5410.
(2) Gracy, R. W.; Noltmann, E. A. *J. Biol. Chem.* **1968**, *243*, 4109.
(3) Hardman, K. D.; Agarwal, R. C.; Freiser, M. *J. Mol. Biol.* **1982**, *157*, 69.
(4) Root, R. L.; Durrwachter, J. R.; Wong, C.-H. *J. Am. Chem. Soc.* **1985**, *107*, 2997.
(5) Whitlow, M.; Howard, A. J.; Finzel, B. C.; Poulos, T. L.; Winborne, E.; Gilliland, G. L. *Proteins* **1991**, *9*, 153.
(6) Jenkins, J.; Janin, J.; Rey, F.; Chiadmi, M.; Tilbeurgh, H.; Lasters, I.; Maeyer, M. D.; Belle, D. V.; Wodak, S. J.; Lauwereys, M.; Stanssens, P.; Mrabet, N. T.; Snauwaert, J.; Matthyssens, G.; Lambeir, A.-M. *Biochemistry* **1992**, *31*, 5449.
(7) Zhang, Y.; Liang, J.-Y.; Huang, S.; Ke, H.; Lipscomb, W. N. *Biochemistry* **1993**, *32*, 17.
(8) Xue, Y.; Huang, S.; Liang, J.-Y.; Zhang, Y.; Lipscomb, W. N. *Proc. Natl. Acad. Sci. U.S.A.* **1994**, *91*, 12482.
(9) Lippard, S. J.; Berg, J. M. *Principles of Bioinorganic Chemistry*; University Science Books: Mill Valley, CA, 1994; Chapter 11.
(10) Yano, S. *Coord. Chem. Rev.* **1988**, *92*, 113.
(11) Yano, S.; Otsuka, K. *Metal Ions in Biological Systems*; Marcel Dekker: New York, 1996; Vol. 32, p 27.
(12) Takizawa, S.; Sugita, H.; Yano, S.; Yoshikawa, S. *J. Am. Chem. Soc.* **1980**, *102*, 7969.
(13) Shioi, H.; Yano, S.; Toriumi, K.; Ito, T.; Yoshikawa, S. *J. Chem. Soc., Chem. Commun.* **1983**, 201.
(14) Tsubomura, T.; Yano, S.; Toriumi, K.; Ito, T.; Yoshikawa, S. *Polyhedron* **1983**, *2*, 123.
(15) Tsubomura, T.; Yano, S.; Toriumi, K.; Ito, T.; Yoshikawa, S. *Bull. Chem. Soc. Jpn.* **1984**, *57*, 1833.
(16) Tsubomura, T.; Yano, S.; Toriumi, K.; Ito, T.; Yoshikawa, S. *Inorg. Chem.* **1985**, *24*, 3218.
(17) Yano, S.; Sakai, T.; Toriumi, K.; Ito, T.; Yoshikawa, S. *Inorg. Chem.* **1985**, *24*, 498.
(18) Tanase, T.; Kurihara, K.; Yano, S.; Kobayashi, K.; Sakurai, T.; Yoshikawa, S. *J. Chem. Soc., Chem. Commun.* **1985**, 1562.
(19) Yano, S.; Takizawa, S.; Sugita, H.; Takahashi, T.; Tsubomura, T.; Shioi, H.; Yoshikawa, S. *Carbohydr. Res.* **1985**, *142*, 179.
(20) Ishida, K.; Yano, S.; Yoshikawa, S. *Inorg. Chem.* **1986**, *25*, 3552.
(21) Tanase, T.; Kurihara, K.; Yano, S.; Kobayashi, K.; Sakurai, T.; Yoshikawa, S. *Inorg. Chem.* **1987**, *26*, 3134.
(22) Ishida, K.; Yashiro, M.; Yano, S.; Hidai, M.; Yoshikawa, S. *J. Am. Chem. Soc.* **1988**, *110*, 2015.
(23) Ishida, K.; Nonoyama, S.; Hirano, T.; Yano, S.; Hidai, M.; Yoshikawa, S. *J. Am. Chem. Soc.* **1989**, *111*, 1599.
(24) Ishida, K.; Yashiro, M.; Yano, S.; Hidai, M.; Yoshikawa, S. *J. Chem. Soc., Dalton Trans.* **1989**, 1241.
(25) Tanase, T.; Nouchi, R.; Oka, Y.; Kato, M.; Nakamura, N.; Yamamura, T.; Yamamoto, Y.; Yano, S. *J. Chem. Soc., Dalton Trans.* **1993**, 2645.
(26) Yano, S.; Kato, M.; Shioi, H.; Takahashi, T.; Tsubomura, T.; Toriumi, K.; Ito, T.; Hidai, M.; Yoshikawa, S. *J. Chem. Soc., Dalton Trans.* **1993**, 1699.
(27) Tanase, T.; Yasuda, Y.; Onaka, T.; Yano, S. *J. Chem. Soc., Dalton Trans.* **1998**, 345.

10.1021/ic9809310 CCC: $18.00
Published on Web 06/11/1999

Scheme 1[a]

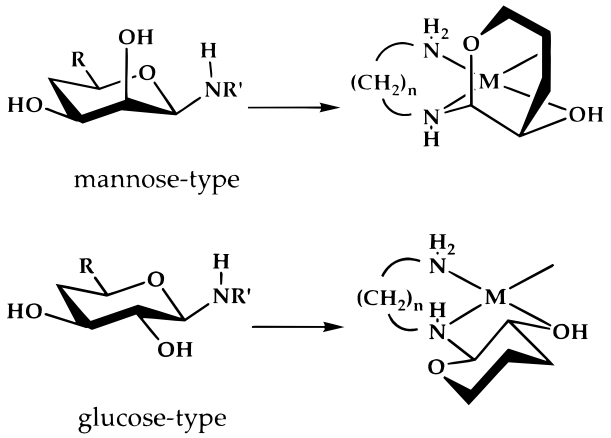

[a] R = CH_2OH, R′ = $-(CH_2)_nNH_2$, n = 2, 3.

in hoping to arrange a highly assembled sugar domain around metal centers,[28−35] which might lead to a minimal model for so-called sugar clusters of glycoproteins playing crucial roles in cell−cell adhesion and recognition.[36−41] We have previously reported the mononuclear cobalt(II) complexes ligated by a heptadentate *N*-glycoside formed from tren and mannose-type aldohexoses, [Co(aldose$_3$-tren)]X_2 (**1**), where aldose$_3$-tren = tris(*N*-aldosyl-2-aminoethyl)amine, aldose = D-mannose (D-Man), L-rhamnose (L-Rha), and X = Cl, Br, $^1/_2SO_4$.[29,31,33] Complex **1** showed a dynamic chiral inversion around the metal center ($\Delta \leftrightarrow \Lambda$) induced by the interaction of the trivalent sugar domain with sulfate anion, which could be regarded as a basic synthetic model for biological induced-fit molecular recognition by a sugar receptor. In general, mannose-type aldoses such as D-Man and L-Rha have 2,3-cis configuration and the sugar ring is axially oriented with respect to the chelate ring upon coordination through the 1,2-functional groups with β-anomeric form (Scheme 1). The axial orientation of D-Man and L-Rha enables close sugar−sugar interactions around metal center.[30] The present study was carried out by utilizing D-glucose (D-Glc) and its disaccharide derivative maltose (Mal) as a sugar part, which has 2,3-trans configuration and was equatorially oriented on ligating through the 1,2-functional groups with β-anomeric form (Scheme 1). The use of the glucose-type sugars has led to an entirely different chemistry from that with the mannose-type sugars and resulted in successful isolation and characterization of novel μ-peroxo dicobalt(III) complexes supported by β-D-glycosyl polyamine ligand, where interligand sugar−sugar hydrogen bonds significantly deviate the $Co_2(\mu\text{-}O_2)$ core from planarity. Further, the clearly observed sugar−sugar interactions of the maltose complex might be of potential importance in relevance to sugar clusters of glycoproteins on the surface of cell membrane. Preliminary results have already been reported.[42]

Experimental Section

Materials. All reagents were of the best commercial grade and were used as received. The following abbreviations are used: tren, tris(2-aminoethyl)amine; D-Glc, D-glucose; Mal, α-D-glucopyranosyl-(1→4)-D-glucose (maltose); D-Man, D-mannose; L-Rha, L-rhamnose (6-deoxy-L-mannose); *N*,*N*′-(aldose)$_2$-tren, bis(*N*-aldosyl-2-aminoethyl)(2-aminoethyl)amine; *N*,*N*′,*N*″-(aldose)$_3$-tren, tris(*N*-aldosyl-2-aminoethyl)amine; *N*-(aldose)-tren, (*N*-aldosyl-2-aminoethyl)bis(2-aminoethyl)amine.

Measurements. Electronic absorption spectra were recorded on a Shimazu UV-3100 spectrometer and circular dichroism spectra on a Jasco J-720 spectropolarimeter. IR spectra were measured on KBr pellets with a JASCO FT/IR-8900μ spectrometer. ^{1}H and ^{1}H−^{1}H COSY NMR spectra were measured in D_2O at 400 and 500 MHz on JEOL GX-400 and Varian Unity 500 plus spectrometers, respectively, and chemical shifts were calibrated with DSS as an internal reference. ^{13}C NMR, ^{13}C−^{1}H COSY, HMBC, and HMQC NMR spectra were measured in D_2O on the spectrometers. Isotopic shifts of ^{13}C NMR spectra were measured in H_2O/D_2O (1/1) mixed solvent at 100 MHz with a broad-band decouple mode.

Preparation of [{Co((D-Glc)$_2$-tren)}$_2$(μ-O_2)]X_3·5H_2O (X = Cl (2·5H_2O), Br (3·5H_2O)). A methanolic solution (300 mL) containing tren (1.32 g, 9.03 mmol), D-glucose (6.50 g, 36.1 mmol) was heated at 63 °C for 80 min. The resultant pale yellow solution was cooled to room temperature, and a methanolic solution of $CoCl_2$·6H_2O (2.15 g, 9.02 mmol) were added to the solution. The reaction mixture was bubbled by dioxygen (or air) for 4 h, the color of which changed from yellow to dark brown, and was allowed to stand at room temperature overnight. The resultant solution was concentrated by a rotary evaporator and was chromatographed on a Sephadex LH-20 gel permeation column (4.5 cm × 65 cm) eluted with methanol. The dark brown main band was collected, and was concentrated to ca. 40 mL to afford brown needle crystals of **2**·5H_2O in 8% yield (440 mg), which were collected by a glass filter, washed with cold methanol and diethyl ether, and dried in vacuo. Slow evaporation of the solution at room temperature afforded block-shaped crystals suitable for X-ray crystallography. Anal. Calcd for $C_{36}H_{85}N_8O_{27}Cl_3Co_2$ (fw 1286.33): C, 33.61; H, 6.66; N, 8.71; Cl, 8.27. Found: C, 33.58; H, 6.43; N, 8.78; Cl, 7.95. UV−vis (in H_2O): ν_{max} (ϵ/10^3) 24.91 (2.87), 41.49 (7.64)^{sh}, 47.39 (9.03)^{sh} ×10^3 cm^{-1} (M^{-1} cm^{-1}). CD (in H_2O): ν_{max} ($\Delta\epsilon$) 18.90 (−8.34), 24.91 (+8.35), 30.86 (+3.29)^{sh}, 38.10 (−5.32), 45.66 (+4.14) (M^{-1} cm^{-1}). IR (KBr): 3356, 1646, 1457, 1419, 1374, 1122, 1082, 1037, 888, 751 cm^{-1}. Complex **3**·5H_2O was prepared by the similar method mentioned above, using tren (0.441 g, 3.02 mmol), D-Glc (2.17 g, 12.1 mmol), and $CoBr_2$·6H_2O (0.984 g, 3.01 mmol). The major dark brown band on a Sephadex LH-20 gel permeation column (4.5 cm × 65 cm) was collected and concentrated to ca. 30 mL. A slow addition of ethanol (5 mL) to the concentrated solution gave brown microcrystals of **3**·5H_2O in 6% yield (128 mg). Anal. Calcd for $C_{36}H_{85}N_8O_{27}Br_3Co_2$ (fw 1419.68): C, 30.46; H, 6.03; N, 7.89; Br, 16.88. Found: C, 30.89; H, 6.22; N, 7.46; Br, 17.15. UV−vis (in H_2O): ν_{max} (ϵ/10^3) 24.88 (3.78), 44.64 (12.1)^{sh} ×10^3 cm^{-1} (M^{-1} cm^{-1}). CD (in H_2O): ν_{max} ($\Delta\epsilon$) 18.87 (−9.47), 24.91 (+9.16), 30.82 (+3.61)^{sh}, 38.17 (−5.24), 45.25 (+3.26). IR (KBr): 3385, 1635, 1460, 1413, 1370, 1264, 1125, 1077, 1037, 888, 751 cm^{-1} (M^{-1} cm^{-1}).

Preparation of [{Co((Mal)$_2$-tren)}$_2$(μ-O_2)]Cl_3·6H_2O (4·6H_2O). A methanolic solution (100 mL) containing tren (0.439 g, 3.00 mmol),

(28) Yano, S.; Takahashi, T.; Sato, Y.; Ishida, K.; Tanase, T.; Hidai, M.; Kobayashi, K.; Sakurai, T. *Chem. Lett.* **1987**, 2153.
(29) Tanase, T.; Nakagoshi, M.; Teratani, A.; Kato, M.; Yamamoto, Y.; Yano, S. *Inorg. Chem.* **1994**, *33*, 6.
(30) Tanase, T.; Doi, M.; Nouchi, R.; Kato, M.; Sato, Y.; Ishida, K.; Kobayashi, K.; Sakurai, T.; Yamamoto, Y.; Yano, S. *Inorg. Chem.* **1996**, *35*, 4848.
(31) Yano, S.; Nakagoshi, M.; Teratani, A.; Kato, M.; Tanase, T.; Yamamoto, Y.; Uekusa, H.; Ohashi, Y. *Mol. Cryst. Liq. Cryst.* **1996**, *276*, 253.
(32) Yano, S.; Doi, M.; Kato, M.; Okura, I.; Nagano, T.; Yamamoto, Y.; Tanase, T. *Inorg. Chim. Acta* **1996**, *249*, 1.
(33) Yano, S.; Nakagoshi, M.; Teratani, A.; Kato, M.; Onaka, T.; Iida, M.; Tanase, T.; Yamamoto, Y.; Uekusa, H.; Ohashi, Y. *Inorg. Chem.* **1997**, *36*, 4187.
(34) Yano, S.; Doi, M.; Tamakoshi, S.; Mori, W.; Mikuriya, M.; Ichimura, A.; Kinoshita, I.; Yamamoto, Y.; Tanase, T. *Chem. Commun.* **1997**, 997.
(35) Tanase, T.; Tamakoshi, S.; Doi, M.; Mori, W.; Yano, S. *Inorg. Chim. Acta* **1997**, *266*, 5.
(36) Stoolman, L. M. *Cell* **1989**, *56*, 907.
(37) Springer, T. A. *Nature* **1990**, *346*, 425.
(38) Misevic, G. N.; Burger, M. M. *J. Biol. Chem.* **1993**, *268*, 4922.
(39) Harmon, R. E. *Cell Surface Carbohydrate Chemistry*; Academic Press: New York, 1978.
(40) Aoki, K.; Ito, K.; Okada, M. *Macromolecules* **1995**, *28*, 5391.
(41) Zanini, D.; Roy, R. *J. Am. Chem. Soc.* **1997**, *119*, 2088.
(42) Tanase, T.; Onaka, T.; Nakagoshi, M.; Kinoshita, I.; Shibata, K.; Doe, M.; Fujii, J.; Yano, S. *Chem. Commun.* **1997**, 2115.

Table 1. Crystallographic and Experimental Data for [{Co((D-Glc)$_2$-tren)}$_2$(μ-O$_2$)]Cl$_3$·4H$_2$O·MeOH (**2**·4H$_2$O·MeOH) and [{Co((Mal)$_2$-tren)}$_2$(μ-O$_2$)]Cl$_3$·2.25H$_2$O·3.75MeOH (**4**·2.25H$_2$O·3.75MeOH)

	2·4H$_2$O·MeOH	**4**·2.25H$_2$O·3.75MeOH
empirical formula	$C_{37}H_{88}N_8O_{27}Co_2Cl_3$	$C_{63.75}H_{134.5}N_8O_{48}Co_2Cl_3$
fw	1301.36	2005.51
cryst syst	orthorhombic	monoclinic
space group	$P2_12_12_1$ (No. 19)	$P2_1$ (No. 4)
a, Å	19.384(8)	12.819(7)
b, Å	23.468(5)	49.160(18)
c, Å	13.195(5)	14.973(6)
β, deg		104.59(4)
V, Å^3	6002(2)	9130(7)
Z	4	4
T, °C	−99	−136
D_{calcd}, g cm^{-1}	1.440	1.459
abs coeff, cm^{-1}	7.71	5.51
2θ range, deg	$3 < 2\theta < 50$	$3 < 2\theta < 45$
no. of unique data	5852	12242
no. of obsd data	4961 ($I > 3\sigma(I)$)	6837 ($I > 2\sigma(I)$)
no. of variables	702	1093
R factors	R^a 0.078	R^a 0.101
	$R_w{}^a$ 0.085	wR^2 ^{b} 0.278

^{a} $R = \sum||F_o| - |F_c||/\Sigma|F_o|$; $R_w = [\sum w(|F_o| - |F_c|)^2/\sum w|F_o|^2]^{1/2}$ ($w = 1/\sigma^2(F_o)$) (for observed data). ^{b} w$R^2 = [\sum w(F_o^2 - F_c^2)^2/\sum w(F_o^2)^2]^{1/2}$ ($w = [\sigma^2(F_o^2) + \{(F_o^2 + 2F_c^2)/30\}^2]^{-1}$) (for all data).

maltose (4.33 g, 12.0 mmol) was heated at 63 °C for 80 min. The resultant pale yellow solution was cooled to room temperature, and a methanolic solution of CoCl$_2$·6H$_2$O (0.714 g, 3.00 mmol) were added to the solution. The reaction mixture was bubbled by dioxygen for 1 h, the color of which changed from yellow to dark brown, and was allowed to stand at room temperature overnight. The resultant solution was concentrated to ca. 60 mL by a rotary evaporator and was chromatographed on a Sephadex LH-20 gel permeation column (4.5 cm × 65 cm) eluted with methanol. The dark brown main band was collected, and was concentrated to <10 mL and small amount of Et$_2$O was added. The solution was kept in refrigerator to afford brown microcrystals of **4**·6H$_2$O in 12% yield (340 mg), which were collected by a glass filter, washed with cold methanol and diethyl ether, and dried in vacuo. Slow evaporation of the solution at room temperature afforded block-shaped crystals suitable for X-ray crystallography. Anal. Calcd for $C_{60}H_{127}N_8O_{48}Cl_3Co_2$ (fw 1952.91): C, 36.90; H, 6.55; N, 5.74; Cl, 5.45. Found: C, 37.04; H, 6.52; N, 5.62; Cl, 5.05. UV−vis (in methanol): ν_{max} (ϵ/10^3) 24.64 (5.43), 44.48 (14.17), ×10^3 cm^{-1} (M^{-1} cm^{-1} metal^{-1}). CD (in methanol): ν_{max} ($\Delta\epsilon$) 18.85 (−11.27), 24.94 (+12.97), 30.30 (+7.95), 40.08 (−7.76), 44.94 (+5.86) (M^{-1} cm^{-1}). IR (KBr): 3398, 1637, 1457, 1419, 1374, 1122, 1147, 1040, 1078 cm^{-1}.

X-ray Crystallography of [{Co((D-Glc)$_2$-tren)}$_2$(μ-O$_2$)]Cl$_3$·4H$_2$O·MeOH and [{Co((Mal)$_2$-tren)}$_2$(μ-O$_2$)]Cl$_3$·2.25H$_2$O·3.75MeOH. Very slow evaporation of the methanolic solutions of **2** and **4** yielded rectangular crystals of **2**·4H$_2$O·MeOH and **4**·2.25H$_2$O·3.75MeOH, which were suitable for X-ray crystallography but extremely delicate when they were separated from the mother liquors. The crystals were quickly coated with Paraton N oil (Exxon) and were mounted on the top of glass fiber at low temperature. Crystal data and experimental conditions are summarized in Table 1. All data were collected at −99 °C (**2**) and −136 °C (**4**) on Rigaku AFC7R diffractometers equipped with graphite monochromated Mo Kα (λ = 0.710 69 Å) radiation. Three standard reflections were monitored every 150 reflections and showed no systematic decrease in intensity. Reflection data were corrected for Lorentz−polarization and absorption effects (ψ scan method).

The structure of **2**·4H$_2$O·MeOH was solved by direct methods with SIR92.[43] The most non-hydrogen atoms were located initially, and subsequent Fourier syntheses gave the positions of other non-hydrogen atoms. The coordinates of C−H and N−H hydrogen atoms were calculated at ideal positions with a distance of 0.95 Å and were not refined. The structure was refined on *F* with the full-matrix least-squares techniques minimizing $\sum w(|F_o| - |F_c|)^2$. Final refinement with anisotropic thermal parameters for non-hydrogen atoms, solvent molecules being refined isotropically, converged at $R = 0.078$ and $R_w = 0.085$, where $R = \sum||F_o| - |F_c||/\sum|F_o|$ and $R_w = [\sum w(|F_o| - |F_c|)^2 / \sum w|F_o|^2]^{1/2}$ ($w = 1/\sigma^2(F_o)$). The three solvent water molecules were disordered. The structure of **4**·2.25H$_2$O·3.75MeOH was solved by direct methods with SIR92. Two independent complex cations, six chloride anions, and 4.5 water and 7.5 methanol solvents were determined in the asymmetric unit. The coordinates of C−H and N−H hydrogen atoms were calculated at ideal positions with a distance of 0.95 Å and were not refined. The structure was refined on F^2 with the full-matrix least-squares techniques minimizing $\sum w(F_o^2 - F_c^2)^2$ with SHELXL93.[44] Final full-matrix least-squares refinement with anisotropic thermal parameters for the Co and Cl atoms and isotropic ones for other non-hydrogen atoms converged at $R = 0.101$ and w$R^2 = 0.278$, where $R = \sum||F_o| - |F_c||/\sum|F_o|$ (for observed data with $I > 2\sigma(I)$) and w$R^2 = [\sum w(F_o^2 - F_c^2)^2/\sum w(F_o^2)^2]^{1/2}$ (for all data, $w = [\sigma^2(F_o^2) + \{(F_o^2 + 2F_c^2)/30\}^2]^{-1}$). One chloride anion (Cl(6), Cl(7)) and two C-6 hydroxymethyl oxygen atoms (O(226), O(227) and O(826), O(827)) were disordered and refined with two sites models. Many solvent molecules are severely disordered, which could be responsible for the relatively high residual values, *R* and wR^2. The absolute configurations of the crystal structures of **2** and **4** were determined by using the known configurations of sugars as internal references.

Atomic scattering factors and values of f' and f'' for Co, Cl, O, N, and C were taken from the literatures.[45,46] All calculations were carried out on a Silicon Graphics Indigo Station with the TEXSAN program package.[47] The perspective views were drawn by using the program ORTEP.[48] Compilation of final atomic parameters for all non-hydrogen atoms is supplied as Supporting Information.

EXAFS Analysis. X-ray absorption measurements around the Co K edge (7000−9200 eV with 780 steps) were performed at the Photon Factory of the National Laboratory for High Energy Physics on beam line 10B using synchrotron radiation (2.5 GeV, 370−300 mA).[49] The experiments were done in the transmission mode on powdered samples of **2** and **4** and a solution sample of **2** (~0.1 M in H$_2$O) using a Si(311) monochromator. The theoretical expression of the obtained $\mathbf{k}^3\chi(\mathbf{k})$ for the case of single scattering is shown in eq 1,

$$\mathbf{k}^3\chi(\mathbf{k}) = \sum_i \left(\frac{\mathbf{k}^2 N_i}{r_i^2} S_i F_i(\mathbf{k}) \exp(-2\sigma_i^2 \mathbf{k}^2) \sin(2\mathbf{k}r_i + \Phi_i(\mathbf{k})) \right) \quad (1)$$

where r_i, N_i, S_i, $F_i(\mathbf{k})$, $\Phi_i(\mathbf{k})$, and σ_i represent the interatomic distance, the coordination number, the reducing factor, the backscattering amplitude, the phase shift, and the Debye−Waller factor, respectively, and $\mathbf{k}$ is the photoelectron wave vector defined as $\mathbf{k} = [(2m/\hbar^2)(E - E_0)]^{1/2}$ (E_0 = 7710 keV).[50] The backscattering amplitude $F_i(\mathbf{k})$ and the phase shift $\Phi_i(\mathbf{k})$ functions used were the theoretical parameters tabulated by McKale et al.[51] Parameters N_i, r_i, E_0, and σ_i were varied in the nonlinear least-squares refined curve fitting with fixed values of S_i. The reducing factors S_i are determined from the analysis of **2** by using fixed N_i values, $N_{N/O} = 6$, $N_C = 8$, and $N_{Co} = 1$. Fourier-filtered (r = 0.8−4.1 Å before phase-shift correction) EXAFS data, $\mathbf{k}^3\chi(\mathbf{k})_{obsd}$, were analyzed with three waves, $\mathbf{k}^3\chi(\mathbf{k})_{calcd} = \mathbf{k}^3\chi_{N/O} + \mathbf{k}^3\chi_C + \mathbf{k}^3\chi_{Co}$, in a $\mathbf{k}$ space of 2.5−15.0 Å^{-1}.[58] The first coordination atoms, 2O + 4N, were treated as oxygen. All calculations were performed on an IBM computer P-120 with the EXAFS analysis program package, REX (Rigaku Co. Ltd.).[52]

(43) Burla, M. C.; Camalli, M.; Cascarano, G.; Giacovazzo, C.; Polidori, G.; Spagna, R.; Viterbo, D. *J. Appl. Crystallogr.* **1989**, *22*, 389.
(44) Sheldrick, G. M. *SHELXL93: Program for the Refinement of Crystal Structures*; University of Göttingen: Germany, 1993.
(45) Cromer, D. T. *Acta Crystallogr.* **1965**, *18*, 17.
(46) Cromer, D. T.; Waber, J. T. *International Tables for X-ray Crystallography*; Kynoch Press: Birmingham, England, 1974.
(47) *TEXSAN Structure Analysis Package*; Molecular Structure Corporation: The Woodlands, TX, 1985.
(48) Johnson, C. K. *ORTEP*; Oak Ridge National Laboratory: Oak Ridge, TN, 1976.
(49) *Photon Factory Activity Report*; National Laboratory for High Energy Physics: Ibaraki, Japan, 1986.
(50) Sayers, D. E.; Stern, E. A.; Lytle, F. W. *Phys. Rev. Lett.* **1971**, *27*, 1204.
(51) McKale, A. G.; Veal, B. W.; Paulikas, A. P.; Chan, S. K.; Knapp, G. S. *J. Am. Chem. Soc.* **1988**, *110*, 3763.

Scheme 2

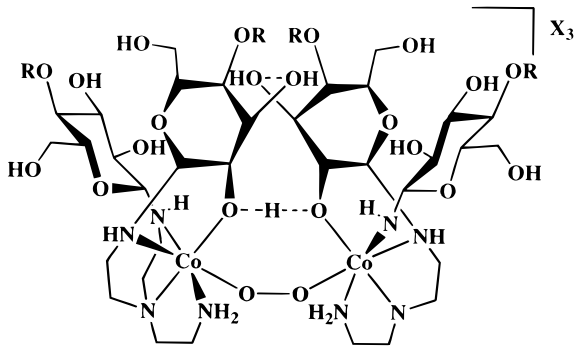

(**2**) R = H, X = Cl
(**3**) R = H, X = Br
(**4**) R = α-D-glucopyranosyl, X = Cl

Molecular Orbital Calculations. Extended Hückel molecular orbital calculations were carried out by using parameters of the Coulomb integrals and the orbital exponents taken from literatures[53−55] on a IBM PC P-120 computer. For the Co d functions, double-ξ expansions were used. The fragment analyses were performed by using program CACAO.[56] Geometrical assumptions were derived from simplifications of the crystal structure of **2**. The model system, $[\{Co(NH_3)_4(H_2O)\}(\mu\text{-}O_2)]^{4+}$, composed of two octahedral *cis*-$[CoN_4O_2]$ units with Co−N = 1.962 Å, Co−O(peroxo) = 1.906 Å, O−O = 1.452 Å, O−H = 0.95 Å, N−H = 1.05 Å, Co−O−O = 117°, and all cis angles being orthogonal.

Results and Discussion

Preparation. Cobalt(II) salts, $Co^{II}X_2{\cdot}6H_2O$ (X = Cl, Br), were treated with bis(*N*-D-glucosyl-2-aminoethyl)amine ((D-Glc)$_2$-tren), which was prepared from D-glucose (D-Glc) and tris(2-aminoethyl)amine (tren) in situ. The reaction mixture was bubbled by dioxygen or air for 4 h and was chromatographed on a Sephadex LH-20 gel permeation column eluted by methanol. Many bands were observed on the column chromatography, and the first-eluted, brown main band was collected. A slow evaporation of the solution yielded brown crystals formulated as $[\{Co((D\text{-}Glc)_2\text{-}tren)\}_2(\mu\text{-}O_2)]X_3{\cdot}5H_2O$ (X = Cl (**2**), Br (**3**)) in low yields, where (D-Glc)$_2$-tren is bis(*N*-D-glucosyl-2-aminoethyl)(aminoethyl)amine (Scheme 2). The similar complex, $[\{Co((Mal)_2\text{-}tren)\}_2(\mu\text{-}O_2)]Cl_3{\cdot}6H_2O$ (**4**), was also isolated, (Mal)$_2$-tren being bis(*N*-maltosyl-2-aminoethyl)(aminoethyl)-amine. The spectroscopic yields of **2**−**4**, determined by UV−vis spectra, were 9−16% based on metal, although the isolated yields were very low. A reaction under nitrogen atmosphere prevented the formation of peroxo-bridged complex, indicating that the peroxo unit is derived from dioxygen, although the reactant of oxygen, presumably cobalt^{II}−*N*-glycoside complex, has not been isolated thus far. The comparatively low yields of the cobalt(III) complexes could be mainly ascribable to the variety of *N*-glycoside ligands in situ; the reaction of tren with 4 equiv of D-glucose provided the (D-Glc)$_2$-tren ligand as a main product as well as (D-Glc)-tren and (D-Glc)$_3$-tren. Complexes **2**−**4** were also prepared by the reaction of cobalt(II) salts with a refluxing mixture of tren and the sugar in a 1:2 ratio, whereas the yields could not be dramatically improved. Elemental analyses indicated that complexes **2**−**4** contained a *N*-glycoside ligand, (aldose)$_2$-tren per metal. In the electronic absorption (AB) spectra (Figure 1), the intense electronic absorption bands (log ϵ 3.46−3.73) were observed around 400 nm, which are corresponding to a peroxo-metal charge-transfer band by analogy with peroxo-bridged Co(III) dinuclear complexes.[57] The IR peaks (**2** and **3**) at 888 cm^{-1} were also assignable to ν_{O-O} vibration. The IR broad bands around 1640 cm^{-1} (δ_{NH}) were characteristic to *N*-glycoside bond formation.[30] The circular dichroism (CD) spectra of **2**−**4** are shown in Figure 1. The CD spectral patterns are closely similar to each other and large Cotton effects are observed around the electronic absorption at 400 nm, strongly indicated that the D-glucosyl moieties are anchored onto the cobalt center. In complex **4**, the nonreducing terminal of maltose, α-D-glucopyranosyl unit, is estimated to be away from the metal, on the basis of AB and CD spectral similarity between the D-glucose and maltose complexes.

NMR Spectroscopy. Complexes **2**−**4** are diamagnetic and could be analyzed by NMR spectroscopic techniques. In general, transition metal complexes with carbohydrates were often fluxional and/or labile owing to low coordination ability of sugar parts and of the sugar-ring opening and closing equilibrium reactions; solid-state structures of metal−sugar complexes were also sometimes entirely different from those of solution state. In this regard, NMR spectroscopic analyses are indispensable and useful to elucidate the solution-state structure of the present complex, which should be compared with its crystal structure. The ^{1}H and ^{13}C NMR spectra of **3**·5H$_2$O in D$_2$O are shown in Figure 2a and b. The assignment was carried out by using ^{1}H−^{1}H COSY, ^{13}C−^{1}H COSY, HMBC, and HMQC techniques (Table 2).[58] Whereas the ^{1}H NMR peaks around δ 3.0−3.9 are severely crowded and the resonance for H2−H5 protons of D-glucose were not clearly identified, the two low-field doublets at δ 4.69 and 4.34 could be assigned to H1 protons of sugars; the small coupling constants, 7.1 and 8.8 Hz, might indicate β-anomeric form. Two H6 protons of the sugars and six methylene protons of tren were observed as AB patterns in the ^{13}C−^{1}H COSY spectrum, Two environmentally different D-glucose moieties were unambiguously confirmed by the ^{13}C NMR spectra, which consists of 12 peaks for the sugars and 6 peaks for the tren ligand. The ^{13}C resonances at δ 93.50 and 90.24 were assigned to the anomeric carbons of D-glucose, which are correlated to the ^{1}H peaks at δ 4.69 and 4.34, respectively, in the ^{13}C−^{1}H COSY spectrum. The assignments of ^{13}C signals for sugars are carried out from the C1 (δ 93.50, 90.24) and C6 (δ 63.39, 61.53) carbons on the basis of the 2D techniques. Although all resonances were assigned as listed in Table 2, the sequences between C2 and C3 carbons of D-glucose could not be determined owing to spectral overlaps. The three aminoethyl arms of tren are chemically nonequivalent with six peaks for C1″−C6″ observed at δ 45.93−65.47 in the ^{13}C NMR spectrum. Since the long-range correlation between the C1′ (δ 90.24) and C4″ (δ 48.18) carbons was observed in the HMQC spectrum, we estimated the linkages of C1′−N−C4″ and C1−N−C2″; the N-glycosidic linkages were confirmed by the deuterium isotope effects in the ^{13}C NMR spectrum (vide infra). These spectral features strongly demonstrated that complex **3** involved bis(*N*-(β-D-glucosyl)aminoethyl)(aminoethyl)amine ligand, (β-D-Glc)$_2$-tren, in an asymmetrical fashion, which is consistent with the crystal structure of **2**.

(52) Kosugi, N.; Kuroda, H. *REX*; Research Center for Spectrochemistry, The University of Tokyo: Tokyo, Japan, 1985.
(53) Hoffmann, R.; Lipscomb, W. N. *J. Chem. Phys.* **1962**, *36*, 3489.
(54) Hoffmann, R. *J. Chem. Phys.* **1963**, *39*, 1397.
(55) Ammeter, J. H.; Burgi, H.-B.; Thibeault, J. C.; Hoffmann, R. *J. Am. Chem. Soc.* **1978**, *100*, 3686.
(56) Mealli, C.; Prosterpio, D. *J. Chem. Educ.* **1990**, *67*, 399.
(57) Solomon, E. I.; Tuczek, F.; Root, D. E.; Brown, C. A. *Chem. Rev.* **1994**, *94*, 827.
(58) Supplied as Supporting Information.

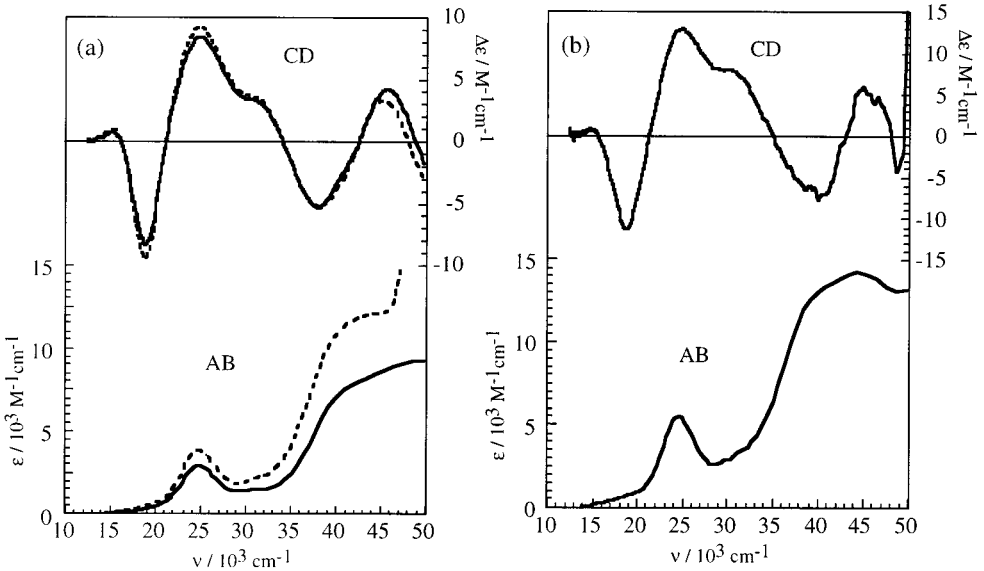

Figure 1. Electronic absorption (AB) and circular dichroism (CD) spectra of (a) [{Co((D-Glc)$_2$-tren)}$_2$(μ-O$_2$)]Cl$_3$·5H$_2$O (**2**·5H$_2$O) (—), [{Co((D-Glc)$_2$-tren)}$_2$(μ-O$_2$)]Br$_3$·5H$_2$O (**3**·5H$_2$O) (- - -), and (b) [{Co(Mal)$_2$-tren)}$_2$(μ-O$_2$)]Cl$_3$·6H$_2$O (**4**·6H$_2$O) (—).

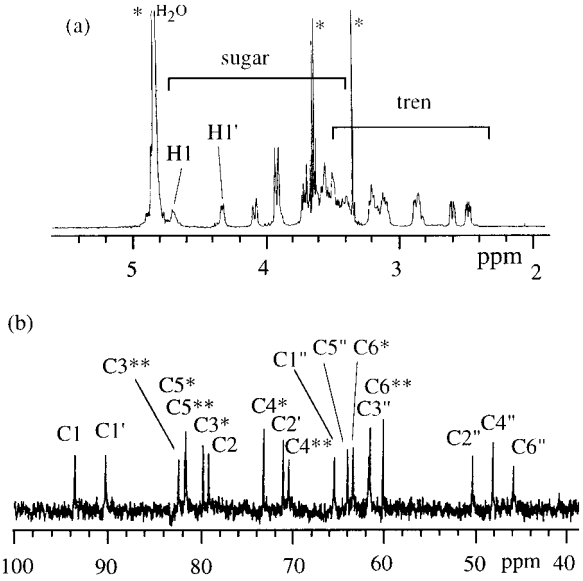

Figure 2. (a) ^{1}H NMR spectrum of [{Co((D-Glc)$_2$-tren)}$_2$(μ-O$_2$)]Br$_3$·5H$_2$O (**3**·5H$_2$O) in D$_2$O, peaks of impurities being marked with asterisk. (b) ^{13}C NMR spectrum of [{Co((D-Glc)$_2$-tren)}$_2$(μ-O$_2$)]Br$_3$·5H$_2$O (**3**·5H$_2$O) in D$_2$O. See Table 2 for the notation of atoms. C3*−C4*−C5*−C6* and C3**−C4**−C5**−C6** correspond to C3−C4−C5−C6 and C3′−C4′−C5′−C6′, respectively, and *vice versa*.

We have previously demonstrated that deuterium isotope effects on ^{13}C NMR chemical shifts are very helpful in spectral assignments and confirmation of N-glycosidic bond formation.[22,24] Partial deuteriation of a coordinated NH_2 primary amino group, existing as NH_2, NHD, and ND_2 in a 1:2:1 ratio, causes ^{13}C resonances of α-carbons to appear as triplets, and that of a NHR secondary amino group, existing as NHR and NDR in a 1:1 ratio, to appear as doublets, since proton exchange of the coordinated amino groups is generally slow on the NMR time scale. The ^{13}C NMR spectrum of **3**·5H$_2$O in a D$_2$O/H$_2$O (1:1) mixed solvent was measured with a broad-band decouple mode. The peaks for the anomeric carbon, C1 and C1′, and α-carbons of tren, C2″, C4″, and C6″, are depicted in Figure 3. The resonances for the C-1 carbon atoms of D-glucose (C1 and C1′) were observed at δ 93.50 and 93.21 as doublets owing to the isotope induced shifts of the neighboring N−H and N−D species. The observed isotope shifts, 95 ppb (C1) and 88 ppb (C1′), are comparable to the values reported as two bond effect.[22,24] These spectral features clearly demonstrated the presence of N-glycosidic bonds between two D-glucose molecules and tren. The resonances for the three methylene carbons

Table 2. ^{13}C NMR Chemical Shifts[a] and Assignments of [{Co((D-Glc)$_2$-tren)}$_2$(μ-O$_2$)]Br$_3$·5H$_2$O (**3**·5H$_2$O)[b]

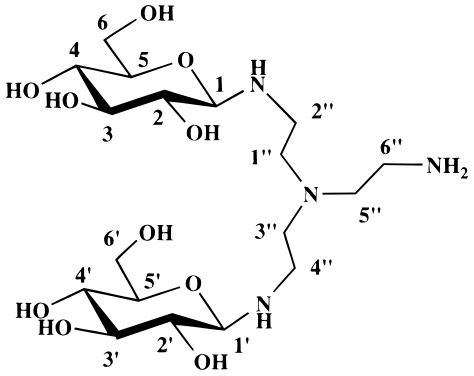

tren part		D-glucose parts					
C1″	−C2″	−C1	−C2	C3/C3′	−C4/C4′	−C5/C5′	−C6/C6′
65.47	50.43	93.50	79.19	79.82	73.25	81.77	63.39
C3″	−C4″	−C1′	−C2′				
61.68	48.18	90.24	71.09	82.46	70.49	81.70	61.53
C5″	−C6″						
64.01	45.93						

[a] In ppm. [b] Measured in D$_2$O at 110 MHz.

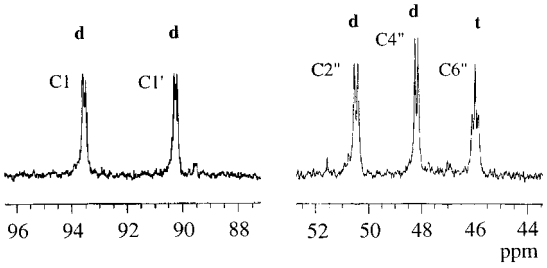

Figure 3. ^{13}C{^{1}H} NMR spectrum of [{Co((D-Glc)$_2$-tren)}$_2$(μ-O$_2$)]-Br$_3$·5H$_2$O (**3**·5H$_2$O) in D$_2$O/H$_2$O (1/1) for the α-carbons with respect to amino groups.

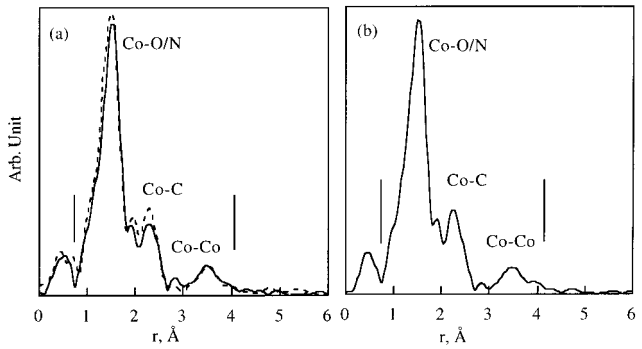

Figure 4. EXAFS Fourier transforms for (a) [{Co((D-Glc)$_2$-tren)}$_2$-(μ-O$_2$)]Cl$_3$·5H$_2$O (**2**·5H$_2$O), powdered sample (—) and solution sample (- - -), and (b) [{Co(Mal)$_2$-tren)}$_2$(μ-O$_2$)]Cl$_3$·6H$_2$O (**4**·6H$_2$O).

(C2″, C4″, C6″) of tren also showed significant isotopic multiplets, two doublets at 50.39 and 48.11 ppm for C2″ and C4″ and a triplet at 45.84 ppm for C6″, which are consistent with an asymmetrical bis(*N*-(D-glucosyl)-2-aminoethyl)(2-aminoethyl)amine ligand. The observed two bond effects per deuterium ($^2\Delta$) are 131 ppb for C2″, 109 bbp for C4″, and 124 ppb for C6″.

The ^{1}H NMR spectrum of **3**·5H$_2$O in DMSO-d_6 showed an extremely low-field shifted proton resonance at δ 12.64.[58] The ^{1}H NMR spectrum of D-glucose and tren in DMSO-d_6 did not exhibit any peaks in lower field below δ ~7, and further, that of the mononuclear cobalt(III) complex with [(Mal)-tren]$^-$ ligand, [Co{(Mal)-tren}Cl]Cl·5H$_2$O (**5**·5H$_2$O),[59] did not exhibit below δ ~7.2.[58] The resonance at δ 12.64 may, thus, correspond to the strongly hydrogen bonded O−H···O$^-$ proton as shown in the X-ray crystal structure of **2** (vide infra).

EXAFS Analyses. EXAFS analysis has been shown to be very useful to determine peroxo-bridged dimetal structures.[60,61] The X-ray absorption spectra around Co K edge were measured for powdered samples of **2** and **4** and for a solution sample of **2** (~0.1 M in H$_2$O),[58] and EXAFS analyses were carried out to determine the local structure around the Co center. The Fourier transforms of the EXAFS data for **2** and **4** are shown in Figure 4. Both spectra are closely similar to each other, and three distinct peaks were observed at about 1.6, 2.5, and 3.8 Å (before phase-shift correction), which were assigned to the backscattering contributions of the nitrogen and oxygen atoms (N/O) coordinating to cobalt, the carbon atoms (C) including five-membered chelate rings, and the outer cobalt atom (Co), respectively, by Fourier filtered pre-curve-fitting analyses. The long-distant Co peak (3.8 Å) were weak but meaningful in the subsequent curve-fitting analyses. The N and O atoms involved in the first coordination sphere were not able to be distinguished in the present analyses. The Fourier filtered (r = 0.8−3.9 Å) EXAFS data, $\mathbf{k}^3\chi(\mathbf{k})_{obsd}$, were subject to curve-fitting analyses with a three-wave model, $\mathbf{k}^3\chi(\mathbf{k})_{calcd} = \mathbf{k}^3\chi(\mathbf{k})_{N/O} + \mathbf{k}^3\chi(\mathbf{k})_C + \mathbf{k}^3\chi(\mathbf{k})_{Co}$ (Figure 5). The structural parameters derived from

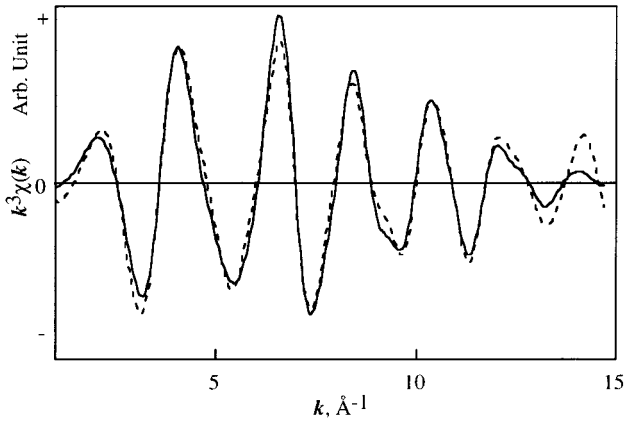

Figure 5. Result of curve-fitting analysis for **2**·5H$_2$O (powdered sample), Fourier-filtered observed data $\mathbf{k}^3\chi(\mathbf{k})_{obsd}$ (—) and calculated data $\mathbf{k}^3\chi(\mathbf{k})_{calcd}$ (- - -).

EXAFS analyses are summarized in Table 3, showing that complexes **2** (D-glucose) and **4** (maltose) are identical to each other at least in the dinuclear framework. The long Co−Co distances (4.06 Å) are consistent with the peroxo-bridge dicobalt structure previously estimated, and further, the Co−O−O−Co dihedral angles could be calculated as ca. 100° by a modeling with the EXAFS parameters (Co···Co = 4.06 Å, Co−O = 1.95 Å), a typical O−O single bond distance of 1.45 Å, and a Co−O−O angle of 115°. The Co−O−O−Co core is assumed to be unusually twisted in comparison with the reported values with L$_5$Co^{III}−O−O−Co^{III}L$_5$ structures (145−180°).[62,63] It should also be notable that both the solid and solution state structures of **2** are almost identical from the EXAFS analysis for its solution sample (Figure 4a and Table 3). Kitajima et al. have carried out a similar procedure of EXAFS analysis on a solution sample of the peroxo-bridged diiron(III) complex, [Fe$_2$(μ-O$_2$)(O$_2$CPh)$_2$-{HB(3,5-*i*Pr$_2$pz)$_3$}$_2$], to predict its structural parameters of Fe···Fe = 4.33 Å, Fe−O = 1.90 Å, and Fe−O−O−Fe torsional angle = ~90°.[60] After its publication, Kim and Lippard have determined the crystal structure of its analogous complex, [Fe$_2$(μ-O$_2$)(μ-O$_2$CCH$_2$Ph)$_2${HB(3,5-*i*Pr$_2$pz)$_3$}$_2$], in which average Fe···Fe separation is 4.004 Å and the average Fe−O−O−Fe dihedral angle is 52.9°. [61] The inconsistency of their structural parameters may arise from a structural difference between in solution and in solid states, for example, owing to the chelating and bridging coordination modes of carboxylate ligands,[60,61] although the EXAFS analysis involved low accuracy in the outer sphere >3 Å. In the present analysis, the close spectral similarity between the solid and the solution samples of **2** indicated a reliability of our prediction on an unusually twisted Co−O−O−Co structure in solution.

Crystal Structures of [{Co((D-Glc)$_2$-tren)}$_2$(μ-O$_2$)]Cl$_3$·4H$_2$O·MeOH (2·4H$_2$O·MeOH) and [{Co(Mal$_2$-tren)}$_2$(μ-O$_2$)]-Cl$_3$·2.25H$_2$O·3.75MeOH (4·2.25H$_2$O·3.75MeOH). ORTEP diagrams for the complex cation of **2** are illustrated in Figure 6a and b, and selected bond distances and angles are listed in Table 4. The asymmetric unit contains a dicobalt complex cation, three chloride anions, and four water and one methanol solvent molecules. The complex cation consists of two Co(III) ions bridged by a peroxo unit (O(1)−O(2) = 1.452(10) Å). The cation has a pseudo C_2 symmetry with respect to an axis passing through the middle of O−O bond. The metal−metal separation

(59) Preparation and characterization of the mononuclear cobalt(III) complex, [Co{(Mal)-tren}Cl]Cl·5H$_2$O (**5**·5H$_2$O), will be reported elsewhere. The structure of the complex was determined by X-ray crystallography to consist of mononuclear Co(III) ion ligated by a chloride anion and a pentadentate (Mal)-tren *N*-glycoside ligand in octahedral geometry (see Supporting Information). The (Mal)-tren ligand coordinated to the metal through the four N atoms of tren residue and the deprotonated C-2 hydroxyl group of maltose moiety.

(60) Kitajima, N.; Tamura, N.; Amagai, H.; Fukui, H.; Moro-oka, Y.; Mizutani, Y.; Kitagawa, T.; Mathur, R.; Heerwegh, K.; Reed, C. A.; Randall, C. R.; Que, L., Jr.; Tatsumi, K. *J. Am. Chem. Soc.* **1994**, *116*, 9071.

(61) Kim, K.; Lippard, S. J. *J. Am. Chem. Soc.* **1996**, *118*, 4914.

(62) Jones, R. D.; Summerville, D. A.; Basolo, R. *Chem. Rev.* **1979**, *72*, 139.

(63) Niederhoffer, E. C.; Timmons, J. H.; Martell, A. E. *Chem. Rev.* **1984**, *84*, 137.

Table 3. Structural Parameters Derived from EXAFS Analyses

compound[a]	shell	A-B[a]	N[b,h]	*r*, Å[c]	σ, Å[d]	ΔE[e]	*R*, %[f]
$[\{Co((D\text{-}Glc)_2\text{-}tren)\}_2(\mu\text{-}O_2)]Cl_3\cdot 5H_2O$	1st	Co-O/N	6[h]	1.95	0.052	2.5	0.040
(**2**·5H$_2$O, powder)			(6)[g]	(1.952)[g]			
	2nd	Co-C	8[h]	2.83	0.055	−0.6	
			(8)[g]				
	3rd	Co-Co	1[h]	4.06	0.080	−21.8	
			(1)[g]	(4.114)[g]			
$[\{Co((D\text{-}Glc)_2\text{-}tren)\}_2(\mu\text{-}O_2)]Cl_3\cdot 5H_2O$	1st	Co-O/N	6.2	1.95	0.059	2.7	0.049
(**2**·5H$_2$O, solution)	2nd	Co-C	9.3	2.82	0.063	−6.2	
	3rd	Co-Co	1.3	4.08	0.101	−20.9	
$[\{Co(Mal_2\text{-}tren)\}_2(\mu\text{-}O_2)]Cl_3\cdot 6H_2O$	1st	Co-O/N	6.1	1.95	0.053	2.7	0.041
			(6)[k]	(1.95)[k]			
(**4**·6H$_2$O, powder)	2nd	Co-C	9.4	2.81	0.065	−6.9	
			(8)[k]				
	3rd	Co-Co	0.8	4.06	0.073	−21.7	
			(1)[k]	(4.097)[k]			

[a] A, absorbing atom; B, backscattering atom. [b] Coordination number. Estimated error is ±1. [c] Interatomic distance in Å. Estimated error is ±0.03 for the 1st shell and ±0.04 for the 2nd and 3rd shells. [d] Debye−Waller factor. [e] Shift of energy in eV from E_0. [f] $R = [\sum(\mathbf{k}^3\chi_o(\mathbf{k}) - \mathbf{k}^3\chi_c(\mathbf{k}))^2/\sum(\mathbf{k}^3\chi_o(\mathbf{k}))^2]^{1/2}$. $\chi_o(\mathbf{k})$ and $\chi_c(\mathbf{k})$ are Fourier-filtered (Δr =0.8−4.1 Å) and calculated data, respectively. $\mathbf{k}^3\chi_c(\mathbf{k}) = \mathbf{k}^3\chi_{O/N}(\mathbf{k}) + \mathbf{k}^3\chi_C(\mathbf{k}) + \mathbf{k}^3\chi_{Co}(\mathbf{k})$. [g] Values determined by X-ray crystallography. [h] Coordination numbers are referenced to complex **2** (powder).

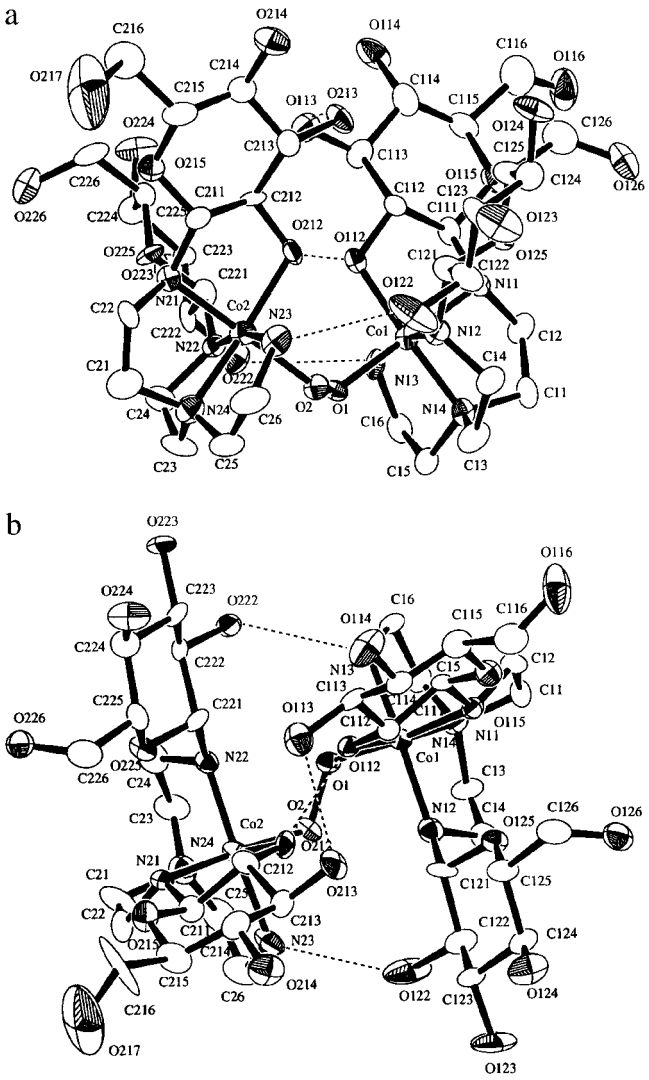

Figure 6. ORTEP plots of the complex cation of **2**, $[\{Co((D\text{-}Glc)_2\text{-}tren)\}_2(\mu\text{-}O_2)]Cl_3$: (a) viewed vertical to the pseudo C_2 axis and (b) viewed along the pseudo C_2 axis.

is 4.114(2) Å. Each cobalt ion is ligated by the *N*-glycoside, (D-Glc)$_2$-tren, through the four nitrogen atoms and the C-2 oxygen atom of a sugar moiety together with the peroxide to form a distorted *cis*-(*O*,*O*)-[CoN$_4$O$_2$] octahedral geometry, trans

Table 4. Selected Bond Distances (Å) and Angles (deg) for **2**·4H$_2$O·MeOH[a]

Bond Distances			
Co(1)··Co(2)	4.114(2)		
Co(1)−O(1)	1.895(7)	Co(1)−O(112)	1.910(7)
Co(1)−N(11)	1.963(9)	Co(1)−N(12)	1.999(9)
Co(1)−N(13)	1.977(8)	Co(1)−N(14)	1.918(9)
Co(2)−O(2)	1.916(7)	Co(2)−O(212)	1.973(7)
Co(2)−N(21)	1.954(9)	Co(2)−N(22)	1.993(9)
Co(2)−N(23)	1.98(1)	Co(2)−N(24)	1.95(1)
O(1)−O(2)	1.452(10)		

Bond Angles			
O(1)−Co(1)−O(112)	92.1(3)	O(1)−Co(1)−N(11)	175.7(3)
O(1)−Co(1)−N(12)	89.8(3)	O(1)−Co(1)−N(13)	81.8(3)
O(1)−Co(1)−N(14)	92.9(3)	O(112)−Co(1)−N(11)	87.6(3)
O(112)−Co(1)−N(12)	97.1(3)	O(112)−Co(1)−N(13)	92.4(3)
O(112)−Co(1)−N(14)	173.8(3)	N(11)−Co(1)−N(12)	94.5(4)
N(11)−Co(1)−N(13)	93.9(4)	N(11)−Co(1)−N(14)	87.2(4)
N(12)−Co(1)−N(13)	167.5(4)	N(12)−Co(1)−N(14)	86.7(4)
N(13)−Co(1)−N(14)	84.6(4)	O(2)−Co(2)−O(212)	92.9(3)
O(2)−Co(2)−N(21)	177.8(4)	O(2)−Co(2)−N(22)	88.9(3)
O(2)−Co(2)−N(23)	81.9(4)	O(2)−Co(2)−N(24)	92.2(4)
O(212)−Co(2)−N(21)	87.2(3)	O(212)−Co(2)−N(22)	97.0(3)
O(212)−Co(2)−N(23)	91.8(4)	O(212)−Co(2)−N(24)	173.2(4)
N(21)−Co(2)−N(22)	93.3(4)	N(21)−Co(2)−N(23)	95.9(4)
N(21)−Co(2)−N(24)	87.6(4)	N(22)−Co(2)−N(23)	167.6(4)
N(22)−Co(2)−N(24)	87.6(4)	N(23)−Co(2)−N(24)	84.4(4)
Co(1)−O(1)−O(2)	118.1(5)	Co(2)−O(2)−O(1)	115.8(5)

[a] Estimated standard deviations are given in parentheses.

and cis angles ranging 168−178° and 82−97°, respectively. Two D-glucopyranosyl units are tethered to a metal center through N-glycosidic bond formation with the amino groups of tren in a β-anomeric form. One of the sugar moieties binds to the metal center through the C-2 hydroxyl oxygen atom and the N-glycosidic nitrogen atom. The other D-glucose residue is anchored on the metal only by the N-glycosidic nitrogen atom; hydroxyl groups of the sugar are away from the coordination sphere of the metal. This coordination mode of *N*-glycoside is unusual and assumed to be unstable concerning the N-glycosidic bond,[32] and however in the present case, the monodentate sugar units could be stabilized by a hydrogen bonding with the primary amino group on the opposite metal center (O(122)···N(23) = 2.95(1) Å, O(222)···N(13) = 2.92(1) Å). The $(\mu\text{-}O_2)Co^{III}_2$ core is further supported by some hydrogen bondings between the sugar moieties (O(112)···O(212) = 2.42(1) Å, O(113)···O(213) = 2.70(1) Å). In particular, the O(112)···O(212) short interatomic distance suggests the presence of O$^-$···H−O type strong

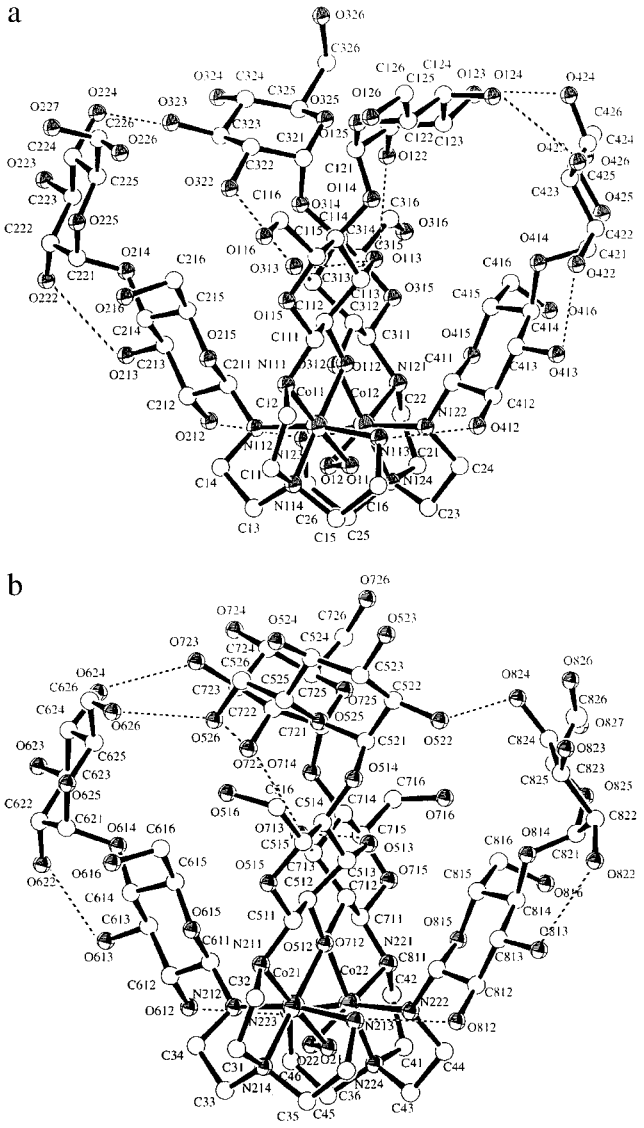

Figure 7. ORTEP plots of the complex cations of **4**, $[\{Co(Mal_2\text{-tren})\}_2(\mu\text{-}O_2)]Cl_3$: (a) cation A and (b) cation B.

hydrogen bond, similar to that observed in the dinuclear Ni(II) complex bridged by β-D-mannofuranoside residue.[18,21] These hydrogen bonding system might deviates the Co−O−O−Co torsional angle from planarity to an intervening, unusual value of 100.4(6)° between 0 and 65° found in $(\mu\text{-}O_2)(\mu\text{-}X)Co^{III}_2$ double-bridged complexes (X = OH, NH) and 145−180° in $(\mu\text{-}O_2)Co^{III}_2$ single-bridged structures.[62−80]

Table 5. Selected Bond Distances (Å) and Angles (deg) for **4**·2.25H_2O·3.75MeOH[a]

cation A		cation B	
Bond Distances			
Co(11)···Co(12)	4.103(5)	Co(21)···Co(22)	4.097(5)
Co(11)−O(11)	1.90(2)	Co(21)−O(21)	1.88(2)
Co(11)−O(112)	1.96(1)	Co(21)−O(512)	1.94(2)
Co(11)−N(111)	1.96(2)	Co(21)−N(211)	1.95(2)
Co(11)−N(112)	2.00(2)	Co(21)−N(212)	1.99(2)
Co(11)−N(113)	1.94(2)	Co(21)−N(213)	1.97(2)
Co(11)−N(114)	1.91(2)	Co(21)−N(214)	1.96(2)
Co(12)−O(12)	1.91(1)	Co(22)−O(22)	1.89(2)
Co(12)−O(312)	1.93(1)	Co(22)−O(712)	1.94(1)
Co(12)−N(121)	1.95(2)	Co(22)−N(221)	1.96(2)
Co(12)−N(122)	2.00(2)	Co(22)−N(222)	2.00(2)
Co(12)−N(123)	1.96(2)	Co(22)−N(223)	1.96(2)
Co(12)−N(124)	1.91(2)	Co(22)−N(224)	1.93(2)
O(11)−O(12)	1.45(2)	O(21)−O(22)	1.47(2)
Bond Angles			
O(11)−Co(11)−O(112)	92.0(6)	O(21)−Co(21)−O(512)	93.4(7)
O(11)−Co(11)−N(111)	177.5(7)	O(21)−Co(21)−N(211)	176.1(8)
O(11)−Co(11)−N(112)	88.7(8)	O(21)−Co(21)−N(212)	88.5(7)
O(11)−Co(11)−N(113)	82.5(8)	O(21)−Co(21)−N(213)	81.1(7)
O(11)−Co(11)−N(114)	92.3(8)	O(21)−Co(21)−N(214)	91.3(7)
O(112)−Co(11)−N(111)	87.3(7)	O(512)−Co(21)−N(211)	87.3(7)
O(112)−Co(11)−N(112)	96.9(6)	O(512)−Co(21)−N(212)	97.3(7)
O(112)−Co(11)−N(113)	90.7(7)	O(512)−Co(21)−N(213)	90.4(8)
O(112)−Co(11)−N(114)	173.1(8)	O(512)−Co(21)−N(214)	173.7(7)
N(111)−Co(11)−N(112)	93.8(9)	N(211)−Co(21)−N(212)	95.2(7)
N(111)−Co(11)−N(113)	95.1(9)	N(211)−Co(21)−N(213)	95.0(7)
N(111)−Co(11)−N(114)	88.3(8)	N(211)−Co(21)−N(214)	87.8(8)
N(112)−Co(11)−N(113)	168.6(8)	N(212)−Co(21)−N(213)	167.5(7)
N(112)−Co(11)−N(114)	88.7(8)	N(212)−Co(21)−N(214)	87.0(8)
N(113)−Co(11)−N(114)	84.4(8)	N(213)−Co(21)−N(214)	86.3(9)
O(12)−Co(12)−O(312)	91.6(6)	O(22)−Co(22)−O(712)	93.8(6)
O(12)−Co(12)−N(121)	177.3(7)	O(22)−Co(22)−N(221)	176.7(7)
O(12)−Co(12)−N(122)	90.1(7)	O(22)−Co(22)−N(222)	89.0(7)
O(12)−Co(12)−N(123)	81.2(7)	O(22)−Co(22)−N(223)	83.2(7)
O(12)−Co(12)−N(124)	93.1(7)	O(22)−Co(22)−N(224)	91.8(7)
O(312)−Co(12)−N(121)	87.9(7)	O(712)−Co(22)−N(221)	87.7(7)
O(312)−Co(12)−N(122)	96.8(7)	O(712)−Co(22)−N(222)	97.2(6)
O(312)−Co(12)−N(123)	91.9(7)	O(712)−Co(22)−N(223)	90.7(6)
O(312)−Co(12)−N(124)	173.2(7)	O(712)−Co(22)−N(224)	172.6(7)
N(121)−Co(12)−N(122)	92.6(7)	N(221)−Co(22)−N(222)	93.8(8)
N(121)−Co(12)−N(123)	96.1(8)	N(221)−Co(22)−N(223)	93.9(8)
N(121)−Co(12)−N(124)	87.1(8)	N(221)−Co(22)−N(224)	86.4(8)
N(122)−Co(12)−N(123)	167.9(6)	N(222)−Co(22)−N(223)	169.3(7)
N(122)−Co(12)−N(124)	88.0(8)	N(222)−Co(22)−N(224)	87.7(7)
N(123)−Co(12)−N(124)	84.1(8)	N(223)−Co(22)−N(224)	85.2(7)
Co(11)−O(11)−O(12)	117(1)	Co(21)−O(21)−O(22)	116(1)
Co(12)−O(12)−O(11)	114(1)	Co(22)−O(22)−O(21)	117(1)

[a] Estimated standard deviations are given in parentheses.

The asymmetric unit of **4**·2.25H_2O·3.75 MeOH involves two dinuclear complex cations, six chloride anions, and 4.5 water and 7.5 methanol molecules. The solvents are considerably disordered in the lattice, which might be responsible for the relatively low-grade refinement. The two complex cations (A and B) are chemically equivalent except the outer sugar domain involving the disorder of the C-6 hydroxymethyl groups (Figure 7a and b). Selected bond distances and angles are listed in Table 5. Here, the structure of cation A is mainly discussed and its ORTEP drawings are illustrated in Figure 8a and b. The structure of the dinuclear core **4**, except the nonreducing α-D-glucopyranosyl residues, is essentially identical to that of **2**. Two cobalt(III) octahedron, ligated by a pentadentate $(Mal)_2$-tren ligand, are bridged by a peroxo unit. The average O−O distance of the peroxo units is 1.46 Å [O(11)−O(12) = 1.45(2) Å, O(21)−O(22) = 1.47(2) Å], and that of Co−Co interatomic distances is 4.100 Å [Co(11)···Co(12) = 4.103(5) Å, Co(21)···Co(22) =

(64) McLendon, G.; Martell, A. E. *Coord. Chem. Rev.* **1976**, *19*, 1.
(65) Schaefer, W. P.; Marsh, R. E. *Acta Crystallogr.* **1966**, *21*, 735.
(66) Christoph, G. G.; Marsh, R. E.; Schaefer, W. P. *Inorg. Chem.* **1969**, *8*, 291.
(67) Thewalt, U.; Marsh, R. E. *Inorg. Chem.* **1972**, *11*, 351.
(68) Thewalt, U. *Z. Anorg. Allg. Chem.* **1972**, *393*, 1.
(69) Shibahara, T.; Mori, M. *Bull. Chem. Soc. Jpn.* **1973**, *46*, 2070.
(70) Yang, C.-H.; Grieb, M. W. *Inorg. Chem.* **1973**, *12*, 663.
(71) Fritch, J. R.; Christoph, G. G.; Schaefer, W. P. *Inorg. Chem.* **1973**, *12*, 2170.
(72) Fronczek, F. R.; Schaefer, W. P.; Marsh, R. E. *Acta Crystallogr.* **1974**, *B30*, 117.
(73) Zehnder, M.; Thewalt, U.; Fallab, S. *Helv. Chim. Acta* **1976**, *59*, 2290.
(74) Thewalt, U.; Struckmeier, G. *Z. Anorg. Allg. Chem.* **1976**, *419*, 163.
(75) Fallab, S.; Zehnder, M.; Thewalt, U. *Helv. Chim. Acta* **1980**, *63*, 1491.
(76) Bigoli, F.; Pellinghelli, M. A. *Cryst. Struct. Commun.* **1981**, *10*, 1445.
(77) Shibahara, T.; Mori, M.; Ooi, S. *Bull. Chem. Soc. Jpn.* **1981**, *54*, 433.
(78) Thewalt, U. *Z. Anorg. Allg. Chem.* **1982**, *485*, 122.
(79) Dexter, D. D.; Sutherby, C. N.; Grieb, M. W.; Beaumont, R. C. *Inorg. Chim. Acta* **1984**, *86*, 19.
(80) Gatehouse, B. M.; Spiccia, L. *Aust. J. Chem.* **1991**, *44*, 351.

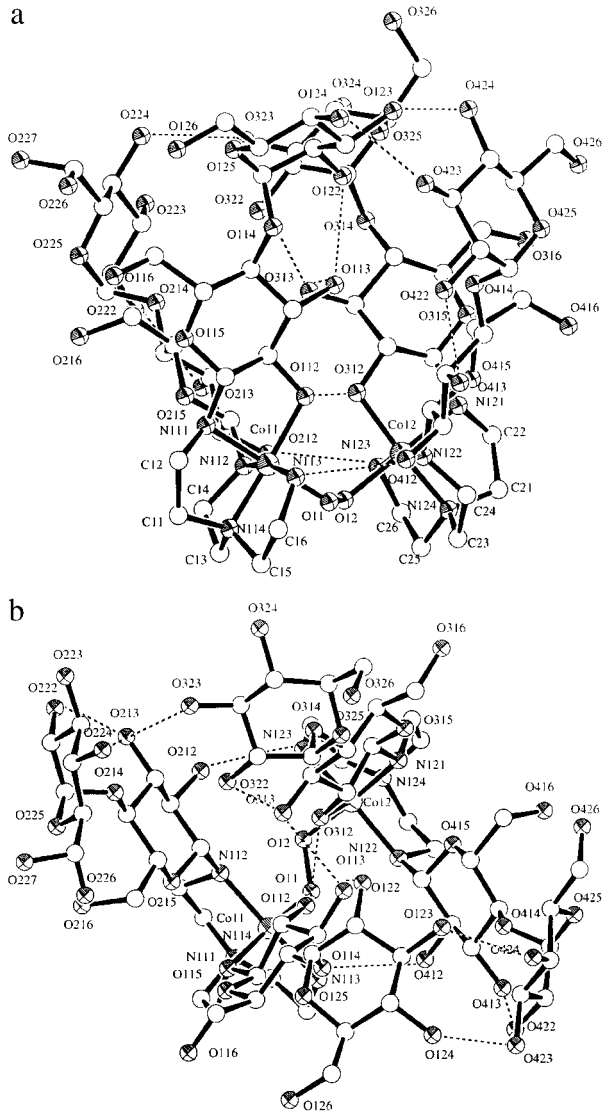

Figure 8. ORTEP plots of the complex cation A of **4**, [{Co(Mal$_2$-tren)}$_2$(μ-O$_2$)]Cl$_3$: (a) viewed vertical to the pseudo C_2 axis and (b) viewed along the pseudo C_2 axis.

4.097(5) Å]. The average Co−O−O−Co torsion angle is deformed to 102°, supported by some interunit hydrogen bonds as observed in **2** [O(112)···O(312) = 2.45(2) Å, O(113)···O(313) = 2.69(2) Å]. Auxiliary inter- and intra-sugar hydrogen bondings are also observed in **4** and are discussed in detail below.

Sugar−Sugar Interactions. Structural elucidation of intermolecular sugar−sugar interactions is extremely important to understand mechanisms for cell−cell adhesions and recognitions and antigen−antibody interactions established by membrane glycoproteins.[36−41,81] However, such structural information has hardly been obtained due to poor crystallization properties of oligosaccharides and unavailability of appropriate small-size model compounds. Complex **4** is able to be recognized as a primitive model compound in which disaccharides are assembled and oriented in a same direction like a shuttle (Figure 9). The complex cation A is discussed in detail, since both cations A and B showed essentially similar orientations and interactions in the nonreducing terminals of the sugars. At first, intra-sugar hydrogen bondings of maltose, between the C-3 hydroxyl group of the reducing terminal unit and C-2′ hydroxyl group of the

(81) Kennedy, J. F.; White, C. A. *Bioactive Carbohydrates in Chemistry, Biochemistry and Biology*; John Wiley & Sons: New York, 1983.

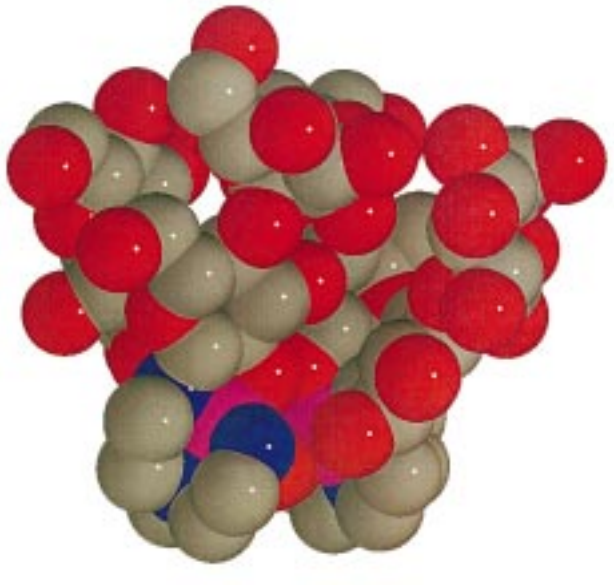

Figure 9. Perspective drawing of the complex cation A of **4**, [{Co((Mal)$_2$-tren)}$_2$(μ-O$_2$)]Cl$_3$, with van der Waals radii: carbon, gray; nitrogen, dark blue; oxygen, red; cobalt, pink.

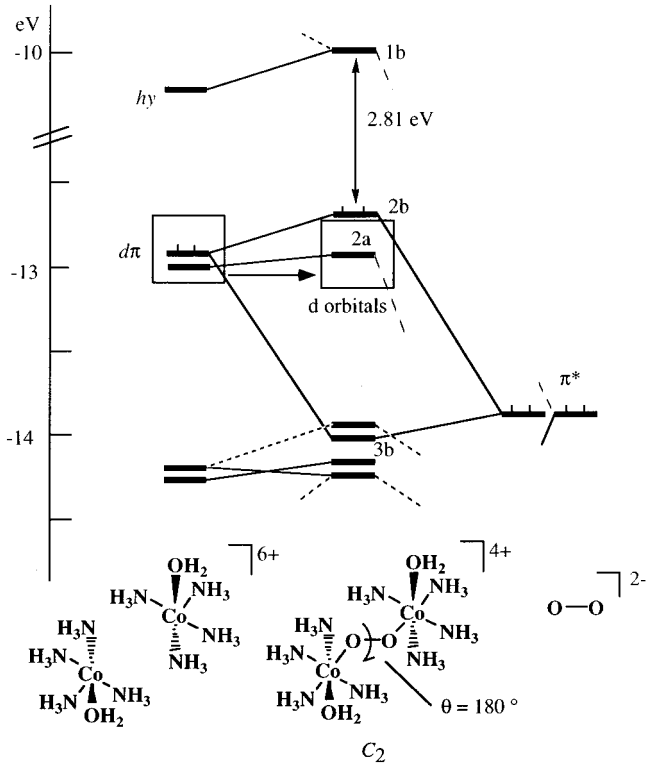

Figure 10. MO interaction diagram for [*cis*-(*O*,*O*)-{Co(NH$_3$)$_4$(H$_2$O)}$_2$-(μ-O$_2$)]$^{4+}$ in terms of 2 [Co(NH$_3$)$_4$(H$_2$O)]$^{3+}$ and O$_2^{2-}$. The torsional angle θ (Co−O−O−Co) is 180°.

nonreducing one, are also observed on the metrical basis of O(113)···O(122) = 2.81(2) Å, O(213)···O(222) = 2.95(2) Å, O(313)···O(322) = 2.76(2), and O(413)···O(422) = 2.74(2) Å. This type of intra-sugar hydrogen bonding of maltose is usual, as is also found in [Ni((Mal)-tn)$_2$]$^{2+}$ (tn = 1,3-diaminopropane) and free maltose,[25] and thus, could be recognized as a main factor to determine the orientation of sugar backbone with α-(1→4)-linkage. The four nonreducing terminals of maltose are loosely bundled by some inter-sugar hydrogen bonding, O(123)···O(424) = 2.59(3) Å, O(124)···O(423) = 2.95(3) Å,

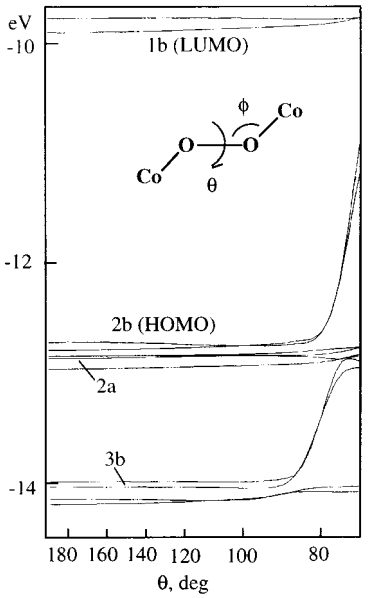

Figure 11. Walsh diagram for the valence MO's of [*cis*-(*O*,*O*)-{$Co(NH_3)_4(H_2O)$}$_2$(μ-O_2)]$^{4+}$ by varying the torsional angle θ (Co−O−O−Co) from 180 to 70° with the Co−O−O angle (ϕ) being 117°.

O(224)···O(323) = 2.66(3) Å, consisting a tetravalent sugar domain regarded as a structurally characterized minimal model for so-called sugar clusters on cell surfaces (Figure 8b).

Molecular Orbital Calculations. To elucidate an electronic structural change by varying Co−O−O−Co torsional angle (θ), extended Hückel MO calculations were performed on a model compound, [*cis*-(*O*,*O*)-{$Co(NH_3)_4(H_2O)$}$_2$(μ-O_2)]$^{4+}$ (**I**) with C_2 symmetry. Figure 10 is an interaction diagram for **I** (θ = 180°) in terms of [{$Co(NH_3)_4(H_2O)$}$_2$]$^{6+}$ and O_2^{2-}, showing a large HOMO 2b (π^*_g)−LOMO 1b (σ^*_u) gap of 2.81 eV which accounts for the stability of (μ-peroxo)dicobalt(III) complexes. A Walsh diagram with the Co−O−O−Co torsion angle θ varying from 180 to 70° is depicted in Figure 11. The energy levels of the valence orbitals are almost independent of θ in the range of 180−95°, while the HOMO (2b) is slightly stabilized around $\theta \sim 100°$ owing to release of the antibonding interaction between the peroxo oxygen atoms. The unstabilization in the range of 95−70° is attributable to repulsive interaction between the water ligands of respective metal center which should be avoided by the sugar−sugar hydrogen bonding [O(112)···O(212)] in **2** and **4**. These results strongly demonstrated that the observed unusually twisted structure (θ = 100−102°) in the $Co_2(\mu$-$O_2)$ core of **2** and **4** is ascribed to a combination of the slight electronic stabilization factor in the $Co_2(\mu$-$O_2)$ core and the sugar−sugar hydrogen bonding interaction.

Conclusion

The peroxo-bridged dicobalt(III) complexes with *N*-glycosides from D-glucose and α-D-glucopyranosyl-(1→4)-D-glucose (maltose), [{Co((aldose)$_2$-tren)}$_2$(μ-O_2)]$^{3+}$, were prepared and characterized by spectroscopic and X-ray analyses to reveal a unusually tilted $Co_2(\mu$-$O_2)$ structure supported by hydrogen bondings within the sugar ligands. The clearly observed sugar−sugar interactions might be of potential importance with relevance to sugar clusters on the surface of cell membrane.[40,41] The present reactions and structures established by glucose-type sugars are also interestingly contrasted with those with the seven-coordinated mononuclear Co(II) complexes with mannose-type sugars, [Co((aldose)$_3$-tren)]$^{2+}$, indicating that the sugar parts dramatically influence the properties of metal center.

Acknowledgment. This work was partially supported by a Grant-in-Aid for Scientific Research from the Ministry of Education of Japan and Grants from Iwatani, Nippon Itagarasu, Mitsubishi-Yuka, and Nagase Foundations, and the San-Ei Gen Foundation for Food Chemical Research.

Supporting Information Available: Tabulations of crystallographic data, and positional and thermal parameters, and bond lengths and angles for **2**·4H_2O·CH_3OH and **4**·2.75H_2O·3.75CH_3OH; ^{1}H−^{1}H and ^{13}C−^{1}H COSY NMR spectra of **3** (Figures S1 and S2); ^{1}H NMR spectra of **3** and **5** in DMSO-d_6 (Figure S3); X-ray absorption spectra, raw EXAFS data, and results of curve-fitting analyses (Figure S4). This material is available free of charge via the Internet at http://pubs.acs.org.

IC9809310